International Symposium
On Turbulence and Shear Flow
Phenomena (TSFP-9)
June 30 - July 3, 2015 Melbourne, Australia

:OUND A SURFACE-MOUNTED SQUARE CYLINDER WITH AR=7

You Qin Wang
High Performance Computing Lab
University of Northern British Columbia
3333 University Way, Prince George, BC, V2M 4Z9, Canada
yqwang@unbc.ca

ABSTRACT

Numerical investigations of flow around a surface-mounted square cylinder of aspect ratio h/d=7 are presented in this paper. The aim is to investigate the effect of the Reynolds number on the flow structure around such a cylinder. Simulations were performed at Reynolds numbers of 130, 652 and 13,041. The results show that the wake structure depends strongly on the Reynolds number. Three different vortex structures are identified with the isosurface of Q, the instantaneous second invariant of the velocity gradient. In the xy-plane, the existence of two spanwise vortices is only observed for the two turbulent cases (Re=652 and Re=13,041). In the laminar case (Re=130), the wake region behind the square cylinder is mainly dominated by both downwash flow and upwash flow. For the two turbulent cases, due to the variations of the strength of the downwash flow, upwash flow and spanwise vortices, two different types of vortex structure were captured. The full-loop shedding is present for the case with a lower Reynolds number, while the half-loop shedding is observed for the case with a higher Reynolds number. Although in all three cases, there is a downwash observed near the free-end and an upwash in the base at the junction, the upwash is strongest in the laminar case, where the upper and lower vortices have similar intensity on the plane of symmetry (y/d=0). For the Re=652 case, a stronger upwash at the junction results in a larger junction vortex than in the case of Re=13,041. It is observed that the strength of the upwash flow decreases when the Reynolds number increases. At Re=13,041, flow structure is mainly dominated by the downwash flow and the spanwise vortex shedding, and the effect of upwash can be ignored.

INTRODUCTION

Turbulent flow around a wall-mounted square cylinder is a subject receiving much attention in the field of wind engineering. Because turbulent flow past bluff bodies involves massive separation and vortex shedding, it presents significant challenges to numerical simulation approaches. Considerable efforts have been made in the past to develop and test various turbulence models, as summarized in an earlier paper by Wang et al. (2014). Among the computational studies on this subject, the one conducted by Chen et al. (2012) should be mentioned. The effect of the boundary layer state on the wake structure of the square cylinder is investigated in their study. They used a laminar solver to model the low Reynolds number case, and LES for the high Reynolds number case. It is interesting to note that for the mean flow, the obstacle wake generated by a laminar oncoming flow is of the quadrupole type, whereas the one generated by a turbulent oncoming flow is of the dipole type. In terms of experimental studies, Wang et al. (2005, 2006, and 2009) have reported a study with h/d ranging from 3-7. They found that the instantaneous flow structure around the square cylinder is similar, regardless of h/d. Meanwhile, experimental investigation conducted by Professor Martinuzzi, as seen in Bourgeois et al. (2011, 2012, and 2013), focused on one aspect ratio of h/d=4. They presented a generalized phase-averaging technique accounting for low-frequency modulation of the base flow, of the oscillation amplitude and frequency, and of higher harmonics. Their methodology goes beyond traditional phase-averaging techniques which identify the flow state with a single phase. The objective of this paper is to investigate the effect of the Reynolds number on the flow structure around a wall-mounted square cylinder.

SIMULATION OVERVIEW

In the present study, the calculation domain was set to be $0.762m \times 0.1778m \times 0.1524m$, and the calculations were performed at three Reynolds numbers based on the width of the square cylinder d and free-stream velocity U_∞. For $Re = 130$, a laminar solver was used to simulate the flow. For Re=652 and Re=13,041, the Reynolds Stress Model (RSM) was used, and mesh schemes were generated having a thin boundary layer around the cylinder walls as well as around the bottom channel wall. More detailed information regarding the RSM used in the present study can be found in a previous paper by Wang et al. (2014b). In the present study, a segregated solution approach using the SIMPLE algorithm was used. The momentum equation was discretized by a second-order upwind scheme. A second-order implicit scheme was used for the unsteady formulation. The non-dimensional time step ($t^* = tU_\infty/d$) was 0.118. At least 4000 time steps were used to obtain the time-averaged results, and convergence was declared when the maximum scaled residuals were less than 10^{-4} for the velocity equations, and less than 10^{-3} for all other equations. Fluid with an approach velocity U_∞ entered the solution domain uniformly at the inlet region, and a no-slip boundary condition was used at the bottom edge. The top edge and both side edges had symmetric boundary conditions. A pressure-

outlet boundary condition was used to define the static pressure at the flow outlet. In addition, the free-stream turbulence intensity was set at 0.04% for $Re = 652$ and 0.8% for $Re = 13,041$.

RESULTS AND DISCUSSTION

Vortex Structure

First of all, in order to compare the vortex structures at three Reynolds numbers, the second invariant of the instantaneous velocity gradient tensor (Q-criterion) is calculated. Q is defined as:

$$Q = (d_{22}d_{33} - d_{23}d_{32}) + (d_{11}d_{22} - d_{12}d_{21}) + (d_{33}d_{11} - d_{13}d_{31}) \quad (1)$$

where

$$\begin{vmatrix} d_{11} & d_{12} & d_{13} \\ d_{21} & d_{22} & d_{23} \\ d_{31} & d_{32} & d_{33} \end{vmatrix} = \begin{vmatrix} \frac{\partial u}{\partial x} & \frac{\partial u}{\partial y} & \frac{\partial u}{\partial z} \\ \frac{\partial v}{\partial x} & \frac{\partial v}{\partial y} & \frac{\partial v}{\partial z} \\ \frac{\partial w}{\partial x} & \frac{\partial w}{\partial y} & \frac{\partial w}{\partial z} \end{vmatrix} \quad (2)$$

Q can be considered to represent the local balance between rotation and strain. A positive Q isosurface represents the area where the strength of strain overcomes rotation. The isosurfaces of the Q for three Reynolds number are shown in Fig. 1. Three different types of vortex structure are observed. In the laminar case, a counter rotating vortex pair, which is nearly symmetric about the x-axis, is present at the upper plane. It is interesting to find that the Q isosurface for Re=130 is very similar with the mean vortex structure identified using the λ_2-criterion in Fig. 8 in the paper by Bourgeois et al. (2011), where λ_2 is the second eigenvalue of the M_{ij} tensor (where $M_{ij} = S_{ik}S_{kj} + \Omega_{ik}\Omega_{kj}, S_{ij} = 1/2(U_{i,j} + U_{j,i})$ and $\Omega_{ij} = 1/2(U_{i,j} - U_{j,i})$). The full-loop structure was observed for Re=652 which is consistent with the similar structure reported for the Re=500 case with $h/d = 4$ (Chen et al., 2012) and the $\delta/h = 0.32$ case with $h/d = 8$ (Hosseini et al., 2012). It should be noted that in both previous studies (Chen et al., 2012 and Hosseini et al., 2012), the coherent vortex structures were identified by the phase-averaged λ_2-criterion (Jeong and Hussain (1995)); however, in the present study, the vortex structure was successfully identified by the instantaneous quantity Q instead of the traditional phase-averaged quantity λ_2. When the Reynolds number increases from 652 to 13,041, the full-loop structure is replaced by the half-loop structure due to the variations in strength of the spanwise vortex, downwash flow, and the upwash flow. The existence of both half-loop and full-loop shedding structures for h/d=7 is consistent with previous studies by Hosseini et al. (2012) for the h/d=8 case. Their study shows that depending on the boundary layer thickness, both of the wake types can form. The shed structures form a half-loop shape for the untripped case (thinner boundary layer) and a full-loop shape for the tripped case (thicker boundary layer). It is obvious that the change of the large-scale vortex structure results from the interaction of the downwash flow, upwash flow, and the spanwise vortex shedding, and that the Reynolds number plays a key role in the shedding process. Instantaneous vertical vorticity contours at $z/d = 1$ are plotted in

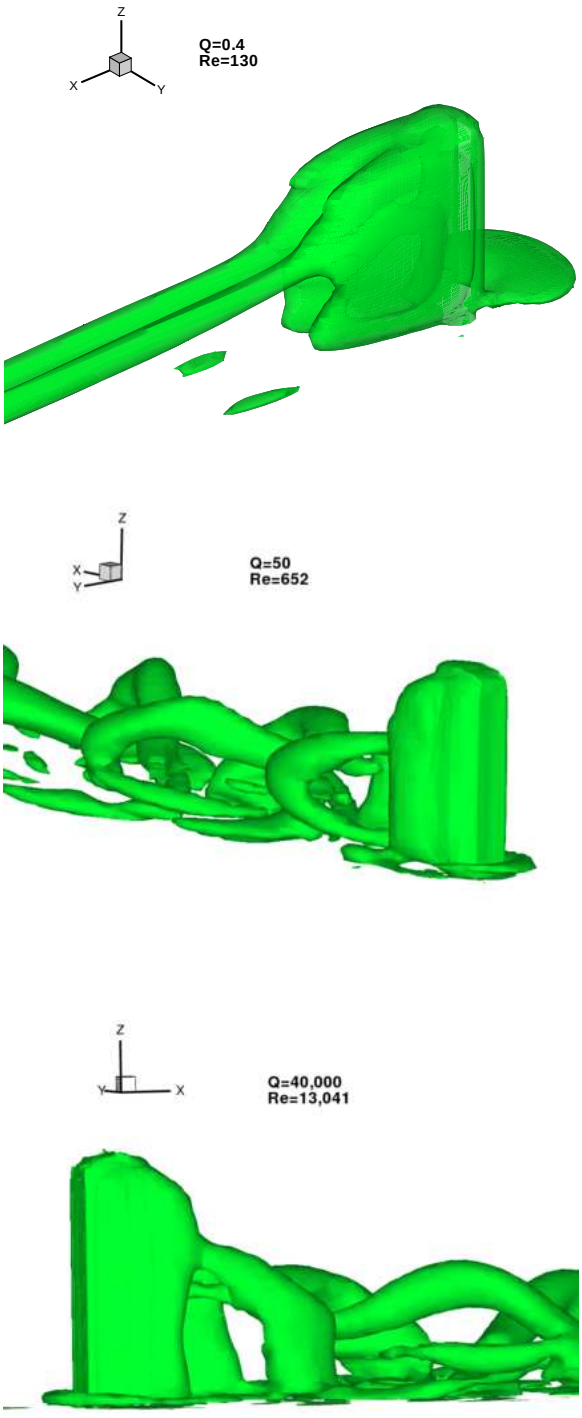

Figure 1. Isosurfaces of instantaneous second invariant of the velocity gradient.

Fig. 2. Vortex shedding is only captured for the two turbulent cases, and vorticity increases as the Reynolds number increases.

Velocity Field

Three different large-scale vortex structures are identified in the previous section, and this section is focused on

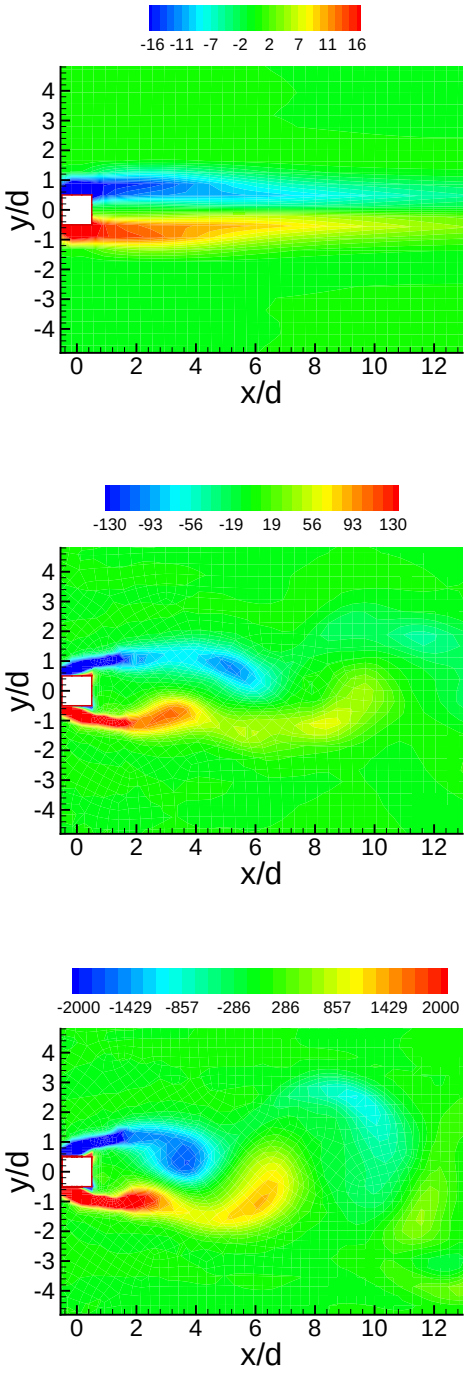

Figure 2. z-vorticity contour at z/d=1: a) Re=130; b) Re=652; c) Re=13,041.

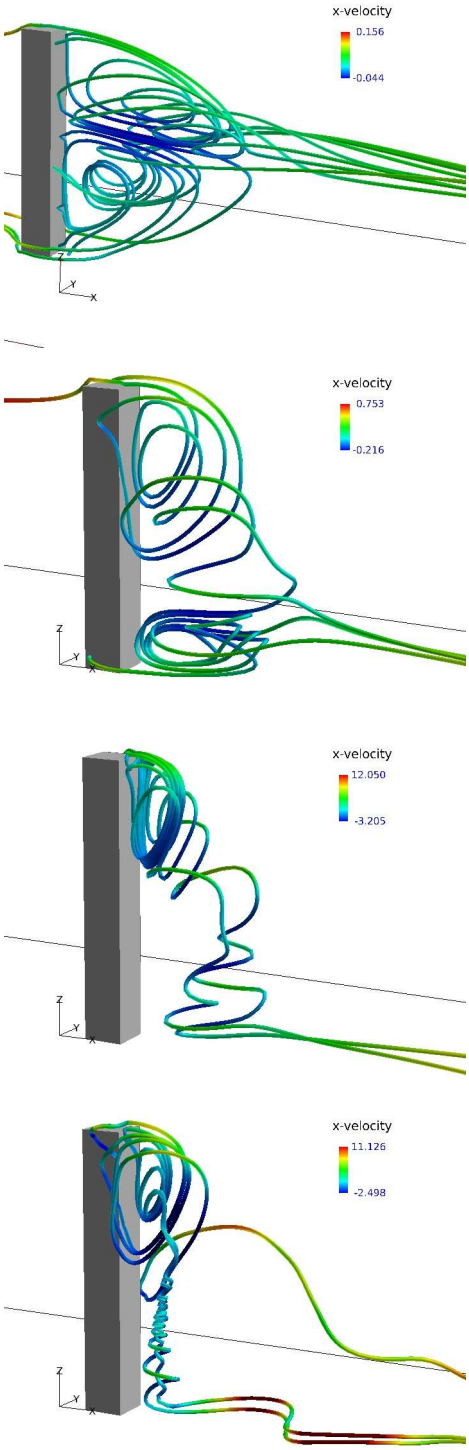

Figure 3. Mean and instantaneous streamlines: a) mean streamlines for Re=130; b) mean streamlines for Re=652; c) mean streamlines for Re=13,041; d) instantaneous streamlines for Re=13,041.

the streamlines around the square cylinder. At Re=130, flow is laminar. The instantaneous streamlines (the plot is not shown here) and the mean streamlines around the square cylinder (see Fig. 3a) are similar. The upwash is strongest in the laminar case, and the upper and lower vortices have similar intensities. For Re=652, although the upwash flow becomes weaker, it still cannot be ignored. In fact, as a result of the interaction of the spanwise vortex shedding and the upwash flow, we see a swirling streamline that starting from the bottom wall, rotates and moves upward, finally reaching approximately 1/4 of the cylinder height before moving downstream. For the Re=13,041 case, the flow is dominated by downwash flow and the vortex shedding. In the instantaneous streamline plot (Fig. 3d), a tornado-like (but upside-down), highly swirling streamline is captured.

The mean streamlines on the plane of symmetry ($y/d = 0$) are plotted in Fig. 4. In the laminar case, the flow is primarily characterized by the interaction of the downwash flow and upwash flow. Three critical points have been ob-

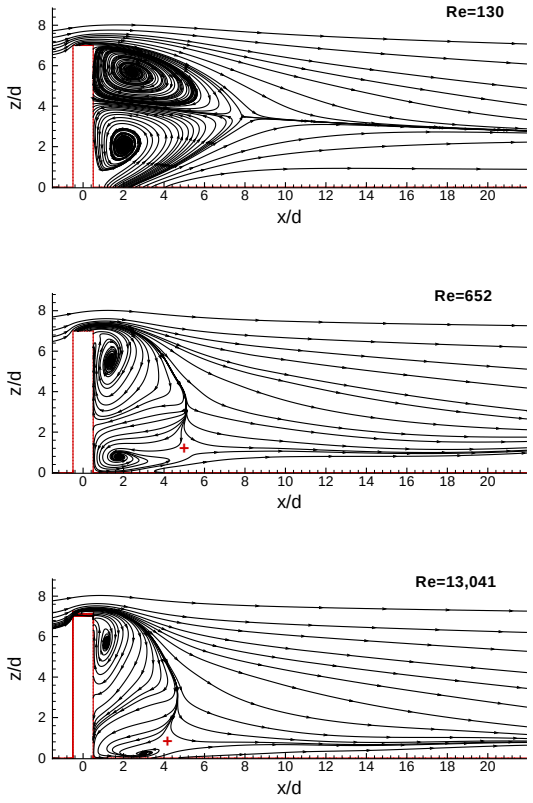

Figure 4. Mean streamlines at y/d=0.

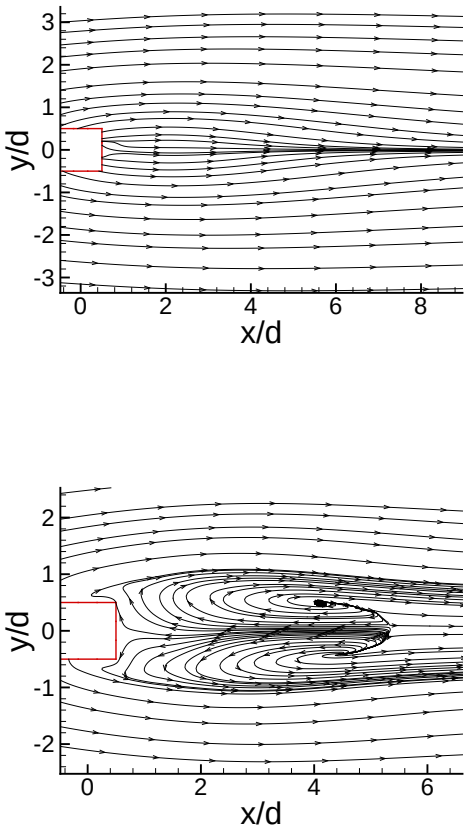

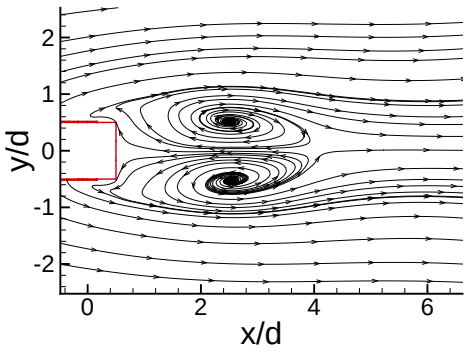

Figure 5. mean streamlines at z/d=1: a) Re=130; b) Re=652; c) Re=13,041.

served, including one saddle point and two foci. The presence of two similar sized counter-rotating vertical structures is associated with two foci, while the saddle point, located near $x/d = 8$, obviously results from the interaction between downwash and upwash flow. The presence of the vortex shedding process at Re=652 and Re=13,041 has tremendously changed flow structures. For turbulence cases, four critical points have been observed, including one saddle point, two foci, and a node. When the Reynolds number increases from 652 to 13,041, the saddle point marked by the symbol + in the figure moves slightly down towards the bottom wall, and the intensity of the lower vortex decreases. For all three cases, there is a large region (upper zone) behind the square cylinder where the flow is dominated by the downwash flow.

Fig. 5 and 6 show the mean streamlines at $z/d = 1$ and $z/d = 3.5$, respectively. The plots reveal that the wake structure behind the square cylinder depends strongly on the Reynolds number. For Re=130, there are no recirculation zones. When the Reynolds number increases from Re=652 to 13,041, the wake tends to become smaller, but stronger. At $z/d = 3.5$, for the laminar case (Re=130), as at $z/d = 1$, there are no recirculation zones. For Re=652, the recirculation region at z/d=1 is slightly larger than that at the mid-span (z/d=3.5), and it further decreases as the elevation increases (the plot at $z/d = 6$ is not shown here). However, for $Re = 13,041$ at mid-span ($z/d = 3.5$), in contrast to what is observed at $z/d = 1$, two parallel vortices with opposite circulations no longer appear in the streamlines plot. Two foci are replaced with one node.

Quasi-Periodical Flow Structure

Part of the temporal evolution of the streamwise drag coefficient on the top wall of the square cylinder for Re=652 and 13,041 are shown in Fig. 7. For Re=652, there is one peak per period, and the drag coefficient is positive. When the Reynolds number increases to 13,041, there are two peaks per period, one slightly higher than the other, and the drag coefficient becomes negative. It indicates the existence of a reverse flow above the top wall of the cylinder. The streamwise drag coefficient converges to a constant (0.038) for the laminar case. The frequency spectra of the stream-

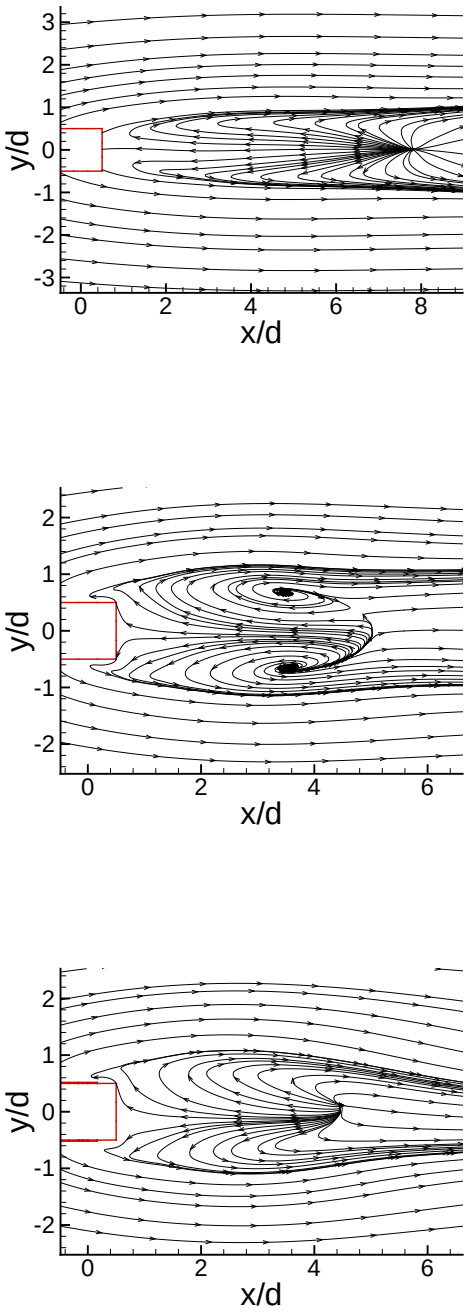

Figure 6. mean streamlines at z/d=3.5: a) Re=130; b) Re=652; c) Re=13,041.

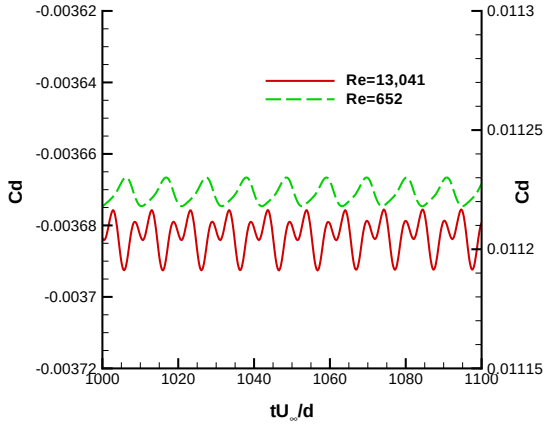

Figure 7. Temporal evolution of the streamwise drag coefficient on the top wall of the square cylinder: Re=652, right y-axis; Re=13,041, left y-axis.

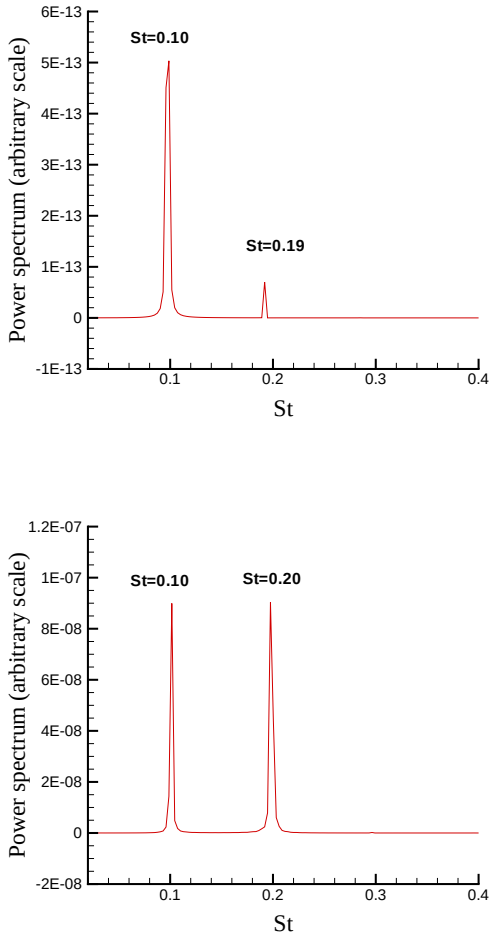

Figure 8. Power spectra of the streamwise drag coefficient: a) Re=652, b) Re=13,041.

wise drag coefficient are shown in Fig. 8. The frequency has been converted to a Strouhal number. The peak value is 0.10 for Re=652, which is consistent with experimental observations obtained by Martinuzzi's group for $h/d = 4$ at a variety of Reynolds numbers, and is slight lower than the value of 0.13 obtained by Wang's group for $h/d = 7$ at Re=9300. Two Strouhal numbers are obtained for Re=13,041: the first is also 0.10, and the second is twice as large.

Conclusions

The flow around a surface-mounted finite square cylinder was simulated by a laminar solver at a Reynolds number of 130, and by the RSM at Reynolds numbers of 652 and 13,041. Some important observations and findings are summarized below:

- The numerical solutions indicate that the flow behind the square cylinder is surprisingly complex, and is highly three-dimensional in all three cases. In the laminar case, the flow is primarily characterized by the interaction of the downwash flow and the upwash flow while for the Re=13,041 case, flow structure is mainly dominated by the downwash flow and the spanwise vortex shedding. At Re=652, the downwash flow, spanwise vortex shedding, and the upwash flow all are important flow features.
- The wake structure behind the square cylinder depends strongly on the Reynolds number. Three different vortex structures are identified: the symmetric, counter rotating vortex pair at Re=130, the alternating full-loop shedding at Re=652, and the alternating half-loop shedding at Re=13,041.
- Q, the instantaneous second invariant of the velocity gradient, is a better analytic measure of the vortex structure than the traditional phase-averaged quantity λ_2 due to its simplicity.
- The strength of upwash flow decreases when the Reynolds number increases while the effect of the Reynolds number on the downwash flow is not obvious.
- Occurrence of alternating spanwise vortex shedding is only observed for the two turbulent cases.
- When the Reynolds number increases from 652 to 13,041, the streamwise drag coefficient on the top wall of the square cylinder changes from positive to negative values, which indicates the existence of a reverse flow above the top wall of the cylinder at Re=13,041.
- Identical vortex shedding frequencies are observed for Re=652 and Re=13,041 ($St = 0.10$). However, for Re=13,041 there is a second St, twice as large in value.

Acknowledgments

The author is grateful for the insight of Dr. Peter L. Jackson. Simulations were performed on a Dell Intel Xeon E5-2690 cluster at the High Performance Computing Lab at the University of Northern British Columbia.

REFERENCES

Bourgeois, J. A., Sattari, P., and Martinuzzi, R. J., 2011, "Alternating Half-Loop Shedding in the Turbulent Wake of a Finite Surface-Mounted Square Cylinder with a Thin Boundary Layer", Physics of Fluids, vol. 23, pp.095101-(1-15).

Bourgeois, J. A., Sattari, P., and Martinuzzi, R. J., 2012, "Coherent Vortical and Straining Structures in the Finite Wall-Mounted Square Cylinder Wake", International Journal of Heat and Fluid Flow, vol. 35, pp.130-140.

Bourgeois, J. A., Noack, B. R., and Martinuzzi, R. J., 2013, "Generalized Phase Average with Applications to Sensor-Based Flow Estimation of the Wall-Mounted Square Cylinder Wake", Journal of Fluids Mechanics, vol. 736, pp.316-350.

Chen, Z., Hosseini, Z., and Martinuzzi, R., 2012, "The influence of boundary layer state on the wake topology of a surface mounted bluff body,",Proceedings, 20th Annual Conference of the Computational Fluid Dynamics Society of Canada, Canmore, Alberta, pp. 1-8.

Hosseini, Z., Bourgeois, J. A., and Martinuzzi, R. J., 2012, "Wall-Mounted Finite Cylinder Wake Structure Modification due to Boundary Layer-Wake Interaction: Half-Loop and Full-Loop Coherent Structure Topologies", Proceedings, 7th International Colloquium on Bluff Body Aerodynamics and Applications, Shanghai, China, pp. 1-10.

Jeong, J., and Hussain, F., 1995, "On the identification of a vortex", Journal of Fluids Mechanics, vol. 285, pp.69-94.

Wang, H. F., Zhou, Y., and Chan, C. K., 2005, "Flow around a Finite Length Square Prism", Proceedings, 4th European & African Conference on Wind Engineering, Prague, Czech Republic, Paper 314, pp. 065106-(1-12).

Wang, H. F., Zhou, Y., Chan, C. K., and Lam, K, S., 2006, "Effect of Initial Conditions on Interaction between a Boundary Layer and a Wall-Mounted Finite-Length-Cylinder Wake", Physics of Fluids, Vol. 18, pp.453-490.

Wang, H. F., and Zhou, Y., 2009, "The Finite-Length Square Cylinder near Wake", Journal of Fluid Mechanics, Vol. 638, pp.453-490.

Wang, Y.Q., Jackson, P. L., and Sui, J., 2012, "Simulation of Flow around a Surface-mounted square-section Cylinder of Aspect Ratio Four", Proceedings, 20th Annual Conference of the Computational Fluid Dynamics Society of Canada, Canmore, Alberta, pp. 1-7.

Wang, Y.Q., and Jackson, P. L., 2014a, "Visualization of Turbulent Flow around a Surface-Mounted Finite Square Cylinder", Proceedings, 6th International Symposium on Computational Wind Engineering, Hamburg, Germany, pp. 1-8.

Wang, Y.Q., Jackson, P. L., and Sui, J., 2014b, "Simulation of Turbulence Flow around a Surface-Mounted Finite Square Cylinder", Journal of Thermophysics and Heat Transfer, Vol. 28, pp. 118-132.